JACS
JOURNAL OF THE AMERICAN CHEMICAL SOCIETY

ARTICLE

pubs.acs.org/JACS

Complexes of Gold(I), Silver(I), and Copper(I) with Pentaaryl[60]fullerides

Merissa Halim, Robert D. Kennedy, Mitsuharu Suzuki, Saeed I. Khan, Paula L. Diaconescu, and Yves Rubin*

Department of Chemistry and Biochemistry, University of California, Los Angeles, California 90095-1569, United States

Supporting Information

ABSTRACT: Gold(I), silver(I), and copper(I) phosphine complexes of 6,9,12,15,18-pentaaryl[60]fullerides **1a** and **1b**, namely, [(4-MeC_6H_4)$_5C_{60}$]Au(PPh_3) (**2a**), [(4-*t*-BuC_6H_4)$_5C_{60}$]Au(PPh_3) (**2b**), [(4-MeC_6H_4)$_5C_{60}$]Ag(PCy_3) (**3a**), [(4-*t*-BuC_6H_4)$_5C_{60}$]Ag(PPh_3) (**3b**), [(4-*t*-BuC_6H_4)$_5C_{60}$]Ag(PCy_3) (**3c**), [(4-MeC_6H_4)$_5C_{60}$]Cu(PPh_3) (**4a**), and [(4-*t*-BuC_6H_4)$_5C_{60}$]Cu(PPh_3) (**4b**), have been synthesized and characterized spectroscopically. All complexes except for **3c** were also characterized by single-crystal X-ray diffraction. Several coordination modes between the cyclopentadienyl ring embedded in the fullerene and the metal centers are observed, ranging from η^1 with a slight distortion toward η^3 in the case of gold(I), to η^2/η^3 for silver(I), and η^5 for copper(I). Silver complexes **3a** and **3b** are rare examples of crystallographically characterized Ag(I) cyclopentadienyls whose preparation was possible thanks to the steric shielding provided by fullerides **1a** and **1b**, which stabilizes these complexes. Silver complexes **3a** and **3b** both display unexpected coordination of the cyclopentadienyl portion of the fulleride anion with Ag(I). DFT calculations on the model systems (H_5C_{60})M(PH_3) and $CpMPH_3$ (M = Au, Ag, or Cu) were carried out to probe the geometries and electronic structures of these metal complexes.

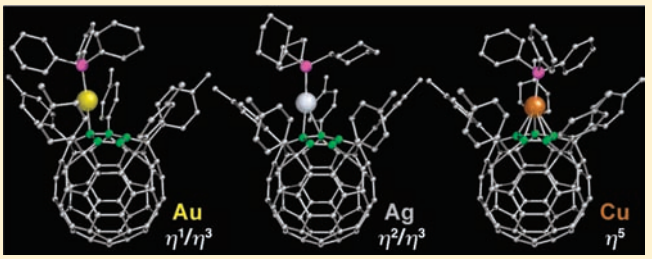

INTRODUCTION

Cyclopentadienyl complexes of the coinage metals are dramatically underrepresented in comparison to those of earlier transition metals. Although only a handful of group 11 metal cyclopentadienyl complexes have been isolated and characterized crystallographically, a range of coordination modes between the cyclopentadienyl ligand and the metal center has nonetheless been observed.[1,3−9] The characterization of group 11 metal cyclopentadienyl compounds, especially of copper and silver, has often been hampered by their instability and high sensitivity to air. These issues have been addressed in some instances by using bulky phosphine or cyclopentadienyl ligands.

The synthesis of a compound with the formula $CpCu\cdot 2[P(n\text{-}Pr)_3]$ was reported in a 1938 patent and describes possibly the first example of a cyclopentadienyl complex of a transition metal element.[1] This copper cyclopentadienyl complex was characterized further and assigned a monohapto-bonded structure after the discovery of ferrocene.[2,3] Pentahapto bonding was suggested following a reexamination of the infrared spectra of $CpCu(PEt_3)$ and $CpCu[P(n\text{-}Bu)_3]$,[4] whose structure was eventually confirmed by X-ray crystallography.[5]

All copper(I) cyclopentadienyl complexes are η^5 coordinated to the Cp ligand, with the exception of the anionic copper(I) cyclopentadienyl complexes $[CuCp_2]^-$ and $[Cu_2Cp_3]^-$, which have slipped-sandwich structures.[6] Neutral cyclopentadienyl copper(I) complexes with a general structure (C_5R_5)Cu(I)L possess stabilizing ligands (L) such as phosphines,[7a,7b] small organometallic clusters,[7c] carbodiphosphoranes,[7d] *N*-heterocyclic carbenes,[7e] alkynes,[7f] and isocyanides.[7g]

In contrast, only seven X-ray structures of neutral gold(I) cyclopentadienyl complexes have been reported.[8] They display atypical coordination modes for cyclopentadienyl transition metal complexes, denoted as η^1/η^3 in this study, and are stabilized exclusively with phosphine ligands. Even more intriguing is the fact that there is only a single example of a crystallographically characterized phosphine-stabilized silver(I) cyclopentadienyl complex, that of $[C_5H_2(SiMe_3)_3]Ag[P(n\text{-}Bu)_3]$. It displays both η^5 and η^3 coordination modes in the crystal.[9]

Over the past decade, the group of Nakamura has developed the organometallic chemistry of the 6,9,12,15,18-pentaarylfulleride (**1**) family, in which coordination to the metal center occurs *via* a cyclopentadienyl ring embedded within the fullerene cage (Chart 1a).[10,11] The thallium(I) complex (η^5-Ph_5C_{60})Tl was the first example of a pentahapto metal−fullerene complex.[12a] Pentamethyl- or pentaarylfulleride complexes with elements of groups 6,[12b] 7,[12c] 8,[12c−i] 9,[12c,j,k] and 10[12l] have since been investigated. Many of these complexes have been characterized crystallographically, revealing η^5 coordination in all cases. Recently, Bouwkamp and Meetsma isolated the discrete ion pair $[Zr(NMe_2)_3(THF)_2][Ph_5C_{60}]$ in an attempt to extend the series to include early transition metals.[12m]

We have become intrigued by the prospect of stabilizing reactive metal complexes or other species with bulky ligands such as the 6,9,12,15,18-pentaarylfulleride anion (**1**). In particular,

Received: February 10, 2011
Published: April 08, 2011

dx.doi.org/10.1021/ja201297r | *J. Am. Chem. Soc.* 2011, 133, 6841–6851

Chart 1. (a) Structure of Pentaarylfulleride Anion 1 with Specific Anions 1a and 1b Used in This Study; (b–d) Complexes of Gold(I) (2a and 2b), Silver(I) (3a, 3b, and 3c), and Copper(I) (4a and 4b) Prepared by Reaction with Corresponding Metal Phosphine Halides; Experimentally Observed Bonding Modes between Fulleride Ligands 1a and 1b and Gold(I), Silver(I), and Copper(I)

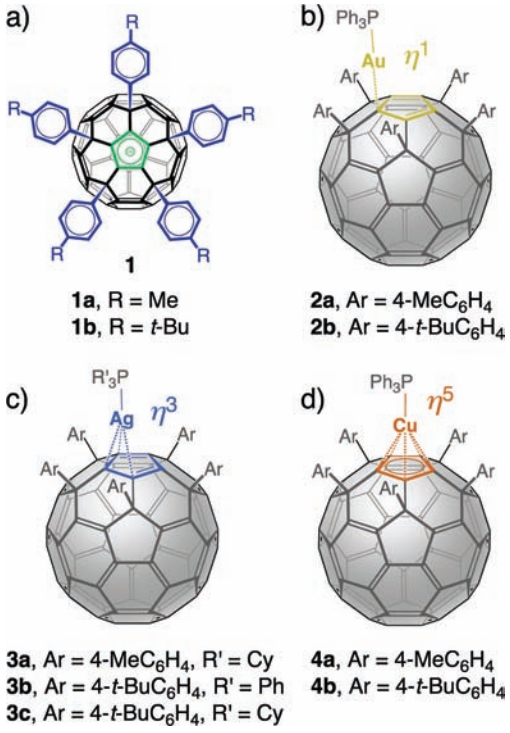

there have been only two reports on the isolation and characterization of pentaarylfulleride complexes of group 11 elements, namely, $(Ph_5C_{60})Cu(PEt_3)$ reported by Sawamura et al.[12a] and the gold(I) complexes $[(4\text{-}MeC_6H_4)_5C_{60}]Au(PPh_3)$ (**2a**) and $[(4\text{-}t\text{-}BuC_6H_4)_5C_{60}]Au(PPh_3)$ (**2b**) reported by us.[13] The latter preliminary communication reported the only example of a crystallographically characterized group 11 metal pentaarylfulleride complex in which a fullerene cage is bonded directly to the metal. The present work extends our investigations and describes the synthesis and crystallographic characterization of the pentaarylfulleride tricyclohexylphosphine complex of silver(I) (**3a**), the corresponding triphenylphosphine complex **3b**, as well as the pentaarylfulleride triphenylphosphine complexes of copper(I) **4a** and **4b**. We make a comparative structural and computational study of these new complexes along with the previously reported phosphine gold(I) complexes **2a** and **2b**.

■ RESULTS AND DISCUSSION

Preparation and Characterization. *Gold(I) Complexes.* To simplify the characterization of reaction products, the pentaaryl-[60]fulleride anions $(4\text{-}MeC_6H_4)_5C_{60}^-$ (**1a**) and $(4\text{-}t\text{-}BuC_6H_4)_5C_{60}^-$ (**1b**) were chosen as ligands owing to the simplicity of the ^1H and ^{13}C NMR spectra of their protonated precursors, as well as the spectra of their corresponding metal complexes. Also, we have found that the corresponding pentaarylfullerenes and their derivatives are particularly crystalline, facilitating characterization by single-crystal X-ray diffraction. Addition of $ClAu(PPh_3)$ to a solution of $K[(4\text{-}MeC_6H_4)_5C_{60}]$ ($\mathbf{1a}\cdot K^+$) in THF followed by purification by chromatography on silica gel afforded $[(4\text{-}MeC_6H_4)_5C_{60}]Au(PPh_3)$ (**2a**) in 70% yield. The *tert*-butyl derivative $[(4\text{-}t\text{-}BuC_6H_4)_5C_{60}]Au(PPh_3)$ (**2b**) was prepared in a similar fashion from $(4\text{-}t\text{-}BuC_6H_4)_5C_{60}^-$ (**1b**) in 95% yield. The

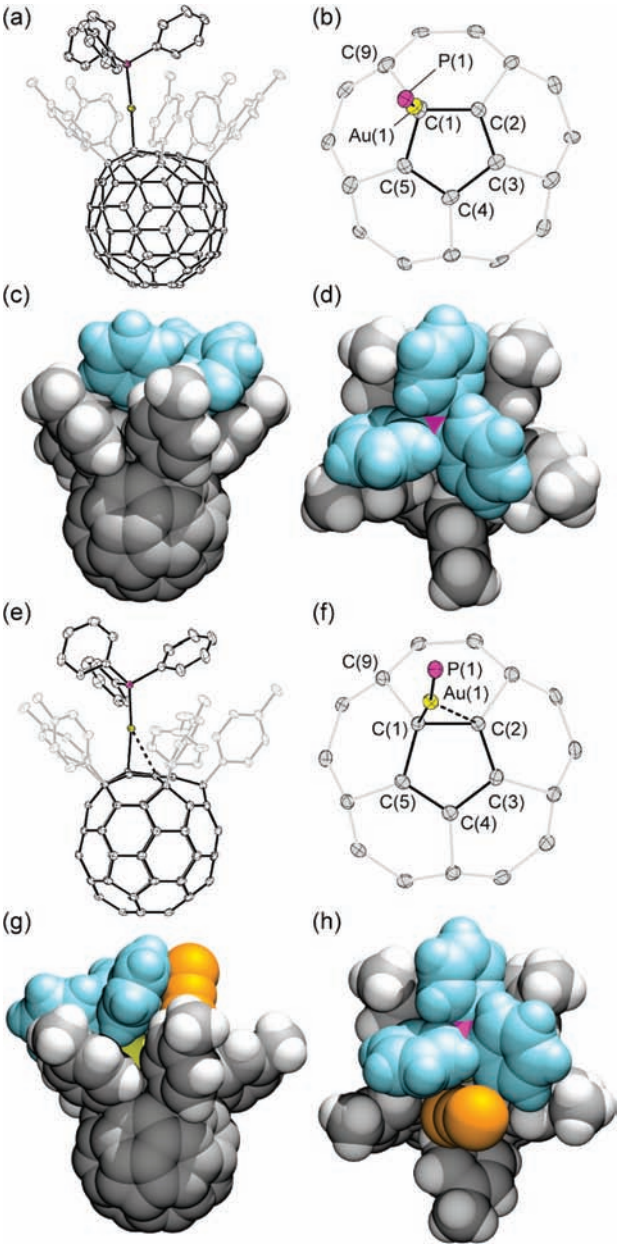

Figure 1. Representations of the crystal structures of $\mathbf{2a}\cdot(ODCB)_2$ (a–d) and $\mathbf{2a}\cdot(CHCl_3)_2(CS_2)$ (e–h). (a) ORTEP drawing (thermal ellipsoids at 50% probability) of compound $\mathbf{2a}\cdot(ODCB)_2$. (b) Partial structure of $\mathbf{2a}\cdot(ODCB)_2$ showing the ligand–metal bonding. (c, d) Space-filling representations of compound $\mathbf{2a}\cdot(ODCB)_2$, viewed approximately perpendicular and parallel to the molecular quasi-C_5 axis. (e) ORTEP drawing (thermal ellipsoids at 50% probability) of compound $\mathbf{2a}\cdot(CHCl_3)_2(CS_2)$. (f) Partial structure of $\mathbf{2a}\cdot(CHCl_3)_2(CS_2)$ showing the metal–ligand bonding. (g, h) Space-filling representations of solvate $\mathbf{2a}\cdot(CHCl_3)_2(CS_2)$, viewed approximately perpendicular and parallel to the molecular quasi-C_5 axis. Hydrogen atoms are omitted for clarity in panels a and e.

dx.doi.org/10.1021/ja201297r | J. Am. Chem. Soc. 2011, 133, 6841–6851

Table 1. Crystallographic Interatomic Distances and Bond Angles for Gold(I) Complexes 2a·$(ODCB)_2$, 2a·$(CHCl_3)_2(CS_2)$, and 2b·$(CHCl_3)_3$; Silver(I) Complexes 3a·$(C_5H_{12})_{0.6}(C_2H_2Cl_4)_3$ and 3b·$(C_4H_8O)_{0.5}(C_6H_6)_{0.5}$ (Molecules A and B); and Copper(I) Complexes 4a·$(CS_2)_3$ and 4b·$(CHCl_3)_3$

	compound							
	2a	**2a**	**2b**	**3a**	**3b(A)**	**3b(B)**	**4a**	**4b**
coordination[a]	η^1/η^3	η^1/η^3	η^1/η^3	η^2/η^3	η^2/η^3	η^2/η^3	η^5	η^5
metal	Au	Au	Au	Ag	Ag	Ag	Cu	Cu
phosphine ligand	PPh_3	PPh_3	PPh_3	PCy_3	PPh_3	PPh_3	PPh_3	PPh_3
included solvent	2 ODCB	2 $CHCl_3$ CS_2	3 $CHCl_3$	0.6 C_5H_{12} 3 $C_2H_2Cl_4$	0.5 THF 0.5 C_6H_6	0.5 THF 0.5 C_6H_6	3 CS_2	3 $CHCl_3$
				Interatomic Distances (Å)				
M(1)−P(1)	2.2602(15)	2.2602(11)	2.254(2)	2.3669(12)	2.3687(14)	2.3830(15)	2.148(8)	2.1570(12)
M(1)−C(1)	2.160(6)	2.176(4)	2.155(7)	2.259(4)	2.288(4)	2.278(5)	2.215(2)	2.224(4)
M(1)−C(2)	2.823(7)	2.590(4)	2.729(9)	2.525(4)	2.464(5)	2.548(5)	2.171(2)	2.318(4)
M(1)−C(3)	3.452(6)	3.377(4)	3.379(8)	3.180(4)	3.224(4)	3.330(5)	2.246(2)	2.345(4)
M(1)−C(4)	3.439(4)	3.592(4)	3.449(8)	3.359(4)	3.503(5)	3.583(5)	2.352(2)	2.281(4)
M(1)−C(5)	2.782(5)	3.050(4)	2.854(8)	2.894(4)	3.051(5)	3.063(5)	2.337(3)	2.190(4)
M(1)−C(9)	3.066(7)	3.039(4)	3.084(8)	3.198(4)	3.157(5)	3.085(5)		
C(1)−C(2)	1.469(7)	1.474(5)	1.494(10)	1.451(5)	1.459(6)	1.460(7)	1.418(3)	1.414(5)
C(2)−C(3)	1.381(8)	1.380(5)	1.374(10)	1.407(6)	1.409(6)	1.405(6)	1.422(3)	1.423(5)
C(3)−C(4)	1.441(8)	1.423(5)	1.425(11)	1.416(5)	1.413(6)	1.419(6)	1.429(3)	1.411(5)
C(4)−C(5)	1.388(7)	1.383(5)	1.381(10)	1.399(5)	1.386(6)	1.395(7)	1.423(3)	1.431(5)
C(5)−C(1)	1.467(8)	1.477(5)	1.477(10)	1.434(5)	1.434(6)	1.442(6)	1.430(3)	1.424(5)
				Bond Angles (deg)				
P(1)−M(1)−C(1)	176.97(16)	172.12(10)	177.3(2)	174.46(10)	168.68(12)	170.67(12)		
M(1)−C(1)−C(2)	100.4(4)	88.2(2)	95.1(5)	82.7(2)	78.8(3)	82.9(3)	69.5(1)	68.3(3)
M(1)−C(1)−C(5)	98.3(4)	111.8(2)	101.9(5)	100.8(2)	107.9(3)	108.8(3)	76.4(1)	73.3(3)
M(1)−C(1)−C(9)	110.6(3)	108.4(2)	111.7(4)	113.8(3)	110.0(3)	106.7(3)	139.2(2)	141.0(3)
				Pyramidalization Angles (θ_p)[b] (deg)				
C(1)	13.5	13.4	13.4	10.2	10.1	10.2	7.3	6.3
C(2)	5.8	5.6	5.9	7.9	7.8	7.9	5.5	6.3
C(3)	5.2	4.3	5.3	5.8	5.5	6.1	6.7	6.8
C(4)	4.5	5.3	4.3	4.8	5.2	5.2	6.8	6.3
C(5)	5.3	6.1	6.1	6.4	6.3	6.4	6.6	7.3
C(1)−C(5) av	6.9	6.9	7.0	7.0	7.0	7.2	6.6	6.6

[a] Coordination of the cyclopentadienide unit in the fulleride ligands **1a** or **1b** with the metal M(1). [b] Pyramidalization angles calculated with the π-orbital axis vector (POAV) model.[14]

^1H and ^{13}C NMR spectra of **2a** and **2b** display signal patterns and intensities corresponding to C_5 symmetry down to −80 °C, which indicates either static pentahapto bonding or fast metallotropic isomerization. Fluxional behavior involving $\eta^1 \rightarrow \eta^2 \rightarrow \eta^1$ isomerization has been reported for other cyclopentadienyl gold(I) phosphine complexes.[8]

Single crystals of **2a** were obtained by slow diffusion of *n*-pentane into a 1,2-dichlorobenzene (ODCB) solution. X-ray diffraction analysis shows that compound **2a** forms a solvate with ODCB and crystallizes in the monoclinic space group *C*2/*c* with **2a**·$(ODCB)_2$ stoichiometry. Representations of the solid-state structure are shown in Figure 1 and crystallographic dimensions as well as diffraction parameters for all compounds except **3c** are presented in Tables 1 and 2. The embedded fullerenyl cyclopentadienyl ring in **2a**·$(ODCB)_2$ displays slightly distorted η^1 coordination to the $Au(PPh_3)$ fragment leaning toward η^3 (denoted η^1/η^3), with a principal Au(1)−C(1) distance of 2.160(6) Å and secondary Au(1)−C(2) and Au(1)−C(5) distances of 2.823(7) and 2.782(5) Å. This coordination mode is characteristic of cyclopentadienyl gold(I) phosphine complexes and is also observed in the related carbaborane anion $[10\text{-}endo(7,8\text{-}nido\text{-}C_2B_9H_{11})Au(PPh_3)]^-$.[15] The principal Au(1)−C(1) bond (2.160(6) Å) is elongated in comparison to a typical Au−C(sp^3) σ bond with no π-bonding contribution such as $MeAu(PPh_3)$ (2.06−2.10 Å).[16] The angles Au(1)−C(1)−C(2) and Au(1)−C(1)−C(5) (100.4(4) and 98.3(4)°, respectively) indicate the approximately symmetrical position of the $Au(PPh_3)$ fragment above carbons C(1), C(2), and C(5) of the fullerene cyclopentadienyl ring. Accordingly, the Au(1)−C(1)−C(9) angle of 110.6(3)° is significantly greater than the Au(1)−C(1)−C(2) and Au(1)−C(1)−C(5) angles (100.4(4) and 98.3(4)°, respectively). Atoms P(1), Au(1), and C(1) are approximately collinear with a P(1)−Au(1)−C(1) angle of 176.97(16)°. The cyclopentadienyl ring is markedly nonplanar with a fold angle of 7.6(6)° between the plane defined by C(1), C(2) and C(5) and the mean plane defined by C(2), C(3), C(4)

dx.doi.org/10.1021/ja201297r |*J. Am. Chem. Soc.* 2011, 133, 6841–6851

Table 2. Selected Single-Crystal X-ray Diffraction Parameters

	complex						
	2a	**2a**	**2b**	**3a**	**3b**	**4a**	**4b**
solvent	$2(C_6H_4Cl_2)$	$2(CHCl_3)$ CS_2	$3(CHCl_3)$	$0.6(C_5H_{12})$ $3(C_2H_2Cl_4)$	$0.5(C_4H_8O)$ $0.5(C_6H_6)$	$3(CS_2)$	$3(CHCl_3)$
formula	$C_{125}H_{58}AuCl_4P$	$C_{116}H_{52}AuCl_6PS_2$	$C_{131}H_{83}AuCl_9P$	$C_{122}H_{81.2}AgCl_{12}P$	$C_{133}H_{87}AgO_{0.5}P$	$C_{116}H_{50}CuPS_6$	$C_{131}H_{83}Cl_{19}CuP$
formula weight	1929.45	1950.33	2203.96	2111.31	1831.87	1730.43	2070.53
description	red platelet	red block	red needle	red prism	red block	red platelet	red block
crystal size (mm^3)	0.13 × 0.07 × 0.04	0.40 × 0.30 × 0.15	0.10 × 0.05 × 0.02	0.20 × 0.12 × 0.06	0.20 × 0.18 × 0.18	0.50 × 0.18 × 0.10	0.14 × 0.08 × 0.03
T (K)	100(2)	100(2)	100(2)	100(2)	100(2)	100(2)	100(2)
radiation	Mo Kα	Mo Kα	Mo Kα	Mo Kα	Mo Kα	Mo Kα	Mo Kα
crystal system	triclinic	monoclinic	triclinic	triclinic	monoclinic	monoclinic	triclinic
space group	$P\bar{1}$	$C2/c$	$P\bar{1}$	$P\bar{1}$	$P2_1/c$	$P2_1/n$	$P\bar{1}$
a (Å)	15.9259(14)	37.699(6)	15.1223(16)	14.227(3)	26.000(4)	17.674(4)	15.9694(13)
b (Å)	16.3684(14)	20.948(4)	15.9245(17)	14.836(3)	24.254(4)	23.521(5)	16.1495(14)
c (Å)	18.8575(16)	20.166(3)	23.844(3)	24.446(5)	28.202(4)	18.549(4)	20.9835(18)
α (deg)	89.7740(10)	90.00	88.4870(10)	73.894(3)	90.00	90.00	81.0180(10)
β (deg)	69.3100(10)	97.111(2)	86.7880(10)	76.732(3)	94.136(2)	96.942(3)	83.4150(10)
γ (deg)	63.8850(10)	90.00	72.517(2)	68.275(3)	90.00	90.00	63.6490(10)
V ($Å^3$)	4061.5(6)	15803(5)	5467.9(11)	4558.6(17)	17738(5)	7655(3)	4783.5(7)
Z	2	8	2	2	8	4	2
ρ_{calcd} ($Mg\cdot m^{-3}$)	1.578	1.640	1.339	1.538	1.372	1.502	1.438
μ (mm^{-1})	2.024	2.198	1.630	0.648	0.305	0.530	0.554
$2\theta_{min}$, $2\theta_{max}$ (deg)	7.34, 56.68	7.60, 58.24	7.28, 56.04	7.56, 58.28	7.40, 52.80	7.48, 58.36	7.28, 56.68
no. refl (unique)	19762	21137	25781	33453	36164	20562	23414
no. refl [$I > 2\sigma(I)$]	12821	17161	16015	24295	19816	13246	9104
R_{int}	0.0984	0.0497	0.1013	0.0	0.0	0.0920	0.0971
$R1$, $wR2$ (all data)	0.1164, 0.1316	0.0615, 0.1228	0.1403, 0.2422	0.1162, 0.2422	0.1470, 0.1983	0.1021, 0.1502	0.1747, 0.1761
$R1$, $wR2$ [$I > 2\sigma(I)$]	0.0616, 0.1113	0.0464, 0.1146	0.0859, 0.2193	0.0879, 0.2190	0.0692, 0.1615	0.0546, 0.1262	0.0661, 0.1453
GOF	0.989	1.101	1.000	1.030	1.019	1.009	0.827
Δ, $e\cdot Å^{-3}$	−1.401, 1.583	−2.759, 2.731	−2.020, 2.412	−2.469, 1.081	−1.205, 0.788	−0.734, 0.507	−1.021, 1.055

and C(5). Atoms C(2), C(3), C(4) and C(5) are sp^2-hybridized and have little pyramidalization, as judged from their π-orbital axis vector angles (POAV, $\theta_p = \theta_{\sigma\pi} - 90$, Table 1),[14] whereas C(1) has appreciable sp^3 character and pyramidalization (13.5°).

The η^1/η^3 coordination and increase in π-bonding relative to a σ-bonded system is further illustrated by comparison of the structure of compound **2a** with that of the previously reported pentaaryl-[60]fullerene $[4\text{-}(EtO_2C)C_6H_4]_5C_{60}Me$, in which a methyl group is purely σ-bonded to the cyclopentadienyl ring.[17] Importantly, the crystal structure of $[4\text{-}(EtO_2C)C_6H_4]_5C_{60}Me$ is atypical in that it shows very little crystallographic disorder, allowing a meaningful analysis of bond lengths and angles within the cyclopentadienyl ring. There is significant bond-length alternation in the cyclopentadienyl ring of compound **2a** (Table 1). The alternation is intermediate between that of a conjugated diene and an aromatic cyclopentadienyl anion. On the other hand, the bond-length alternation within the cyclopentadiene ring of $C_{60}[4\text{-}C_6H_4(CO_2Et)]_5Me$ is significantly larger, with formal single and double bonds of 1.523 and 1.349 Å, respectively.[17] Furthermore, the pyramidalization angle of the sp^3 cyclopentadienyl carbon atom is 17.4° in the latter, which is 3.9° larger than the corresponding carbon atom in compound **2a**, and accordingly reflects its greater sp^3 character. The angles C(2)−C(1)−C(Me) and C(5)−C(1)−C(Me) of $C_{60}[4\text{-}C_6H_4(CO_2Et)]_5Me$ are significantly larger (102.7° and 105.5°, respectively) than those of **2a** (100.4° and 98.3°, respectively), reflecting the contribution of π bonding between the cyclopentadienyl system and the $Au(PPh_3)$ fragment in the gold(I) complex **2a**.

X-ray diffraction analysis was also performed on a single crystal of compound **2a** grown from a $CS_2/CHCl_3$ mixed-solvent system. Under these conditions, compound **2a** crystallizes in the $C2/c$ space group with $\mathbf{2a}\cdot(CHCl_3)_2(CS_2)$ stoichiometry. Similarly to the ODCB solvate, the cyclopentadienyl ring displays η^1/η^3 coordination to gold(I) (Figure 1f). However, there is significant deviation toward η^2 coordination in this case. Although the principal Au(1)−C(1) distance of 2.176(4) Å is nearly identical to that of the ODCB solvate, the secondary interactions Au(1)−C(2) and Au(1)−C(5) are 2.590(4) and 3.050(4) Å, respectively, and the corresponding angles Au(1)−C(1)−C(2) and Au(1)−C(1)−C(5) are 88.2(2)° and 111.8(2)°, illustrating the asymmetry of the metal−ligand coordination. Additionally, a carbon disulfide molecule resides in a narrow cavity between the $Au(PPh_3)$ moiety and an adjacent fullerene-anchored tolyl group, which may be responsible for the observed $\eta^1 \rightarrow \eta^2$ distortion. Although there is significant distortion toward η^2 coordination, the cyclopentadienyl ring in $\mathbf{2a}\cdot(CHCl_3)_2(CS_2)$ has partially localized 1,3-diene character, and the C−C distances are similar to those of solvate $\mathbf{2a}\cdot(ODCB)_2$ (Table 1). This indicates that the $\eta^1 \rightarrow \eta^2$ distortion does not involve a fundamental change in the ligand−metal bonding.

dx.doi.org/10.1021/ja201297r | J. Am. Chem. Soc. 2011, 133, 6841–6851

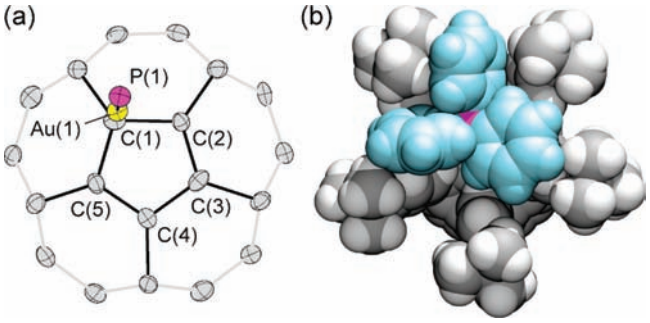

Figure 2. Representations of the crystal structure of **2b**·$(CHCl_3)_3$. (a) ORTEP drawing (thermal ellipsoids at 50% probability) of the partial structure of **2b** showing metal−ligand bonding. (b) Space-filling representation of **2b** viewed along the molecular quasi-C_5 axis.

Finally, X-ray diffraction analysis was also performed on a single crystal of the *tert*-butyl derivative **2b** grown from a CS_2/$CHCl_3$ mixed-solvent system (Figure 2). Under these conditions, compound **2b** forms crystals with **2b**·$(CHCl_3)_3$ stoichiometry. The coordination of the fullerene cyclopentadienyl ring to gold(I) is similar in **2b**·$(CHCl_3)_3$ and **2a**·$(ODCB)_2$, i.e., a nearly symmetrical η^1/η^3 coordination is observed (Figure 2a). The "secondary" interactions Au(1)−C(2) and Au(1)−C(5) (2.729(9) and 2.854(8) Å, respectively) confirm a slight distortion toward η^2 coordination.

The isolobal relationship[18] between the proton and the cationic $Au(PR_3)^+$ fragment can be invoked to outline the bonding observed in complexes **2a** and **2b**.[19] Whereas the vacant, degenerate gold-centered $6p_x$ and $6p_y$ orbitals of the $Au(PR_3)^+$ fragment are too high in energy to interact strongly with the filled cyclopentadienyl-based orbitals of appropriate symmetry, the hybrid $6s/6p_z$ orbital behaves similarly to the vacant 1s orbital of the proton. Pentahapto bonding is disfavored as this would involve destabilizing interactions between the gold(I) 5d orbitals and filled cyclopentadienyl π orbitals. Rather, an energetic compromise is reached with the η^1/η^3 geometry. On the other hand, pentahapto bonding is found in the anionic gold heteroborane clusters $[3\text{-}(PPh_3)\text{-}closo\text{-}2,1\text{-}AuTeB_{10}H_{10}]^-$ and $[3\text{-}(PPh_3)\text{-}closo\text{-}3,1,2\text{-}AuAs_2B_9H_9]^-$, which possess cyclopentadienyl-type ligands with energetically higher-lying molecular orbitals.[20]

Silver(I) Complexes. In the silver(I) series of cyclopentadienyl complexes, the compound $[C_5H_2(SiMe_3)_3]Ag[P(n\text{-}Bu)_3]$ is the only "pristine" Cp−Ag(I) complex present in the literature.[9] The related complexes $\{[(MeO_2C)_5C_5]Ag(PPh_3)\}_2$ and $[(MeO_2C)_5C_5]Ag(PPh_3)_2$ possess η^2-bonded pentakis(methoxycarbonyl)cyclopentadienyl ligands,[21] with silver centers having ester carbonyl groups and water molecules within their coordination sphere that compete with the cyclopentadienyl ligand for binding and interfere with a higher hapticity metal−cyclopentadienyl bonding.

We envisioned that the steric encumbrance of the pentaarylfulleride ligand **1** would provide a particularly stabilizing environment for enhanced metal−cyclopentadienyl bonding by preventing the coordination of other ligands to silver. In addition, silver(I) cyclopentadienyl complexes are notoriously unstable, and the aryl groups of **1a** or **1b** should protect the resulting complexes and allow isolation and characterization.[22] Accordingly, a series of low-temperature reactions using $ClAg(PCy_3)$ with $K[(4\text{-}MeC_6H_4)_5C_{60}]$ (**1a**·K^+) and $ClAg(PPh_3)$ with $K[(4\text{-}t\text{-}BuC_6H_4)_5C_{60}]$ (**1b**·K^+) were carefully carried out, resulting in the formation of the silver(I) phosphine complexes $[(4\text{-}MeC_6H_4)_5C_{60}]Ag(PCy_3)$ (**3a**), $[(4\text{-}t\text{-}BuC_6H_4)_5C_{60}]Ag(PPh_3)$ (**3b**), and $[(4\text{-}t\text{-}BuC_6H_4)_5C_{60}]Ag(PCy_3)$ (**3c**), respectively.[23] Compounds **3a**−**c** were too air-sensitive for purification by chromatography on silica gel. Consequently, they were isolated by removal of THF from the reaction mixture in vacuo, followed by extraction with CS_2 or benzene, and subsequent filtration under argon. Using this method, fractional amounts of (triphenylphosphine)silver(I) chloride were present in the final products before their crystallization, as determined by NMR spectroscopy.

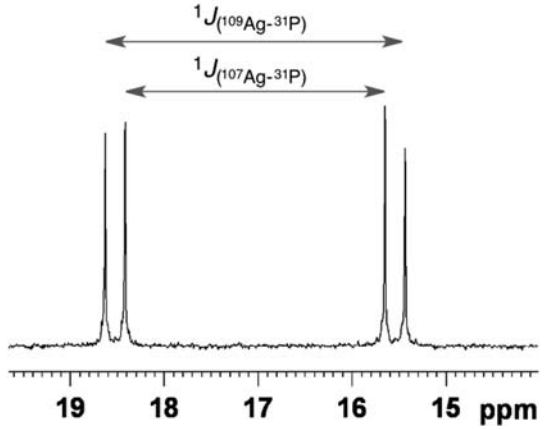

Figure 3. Expansion of the proton-decoupled ^{31}P NMR spectrum of silver(I) complex **3b** showing two doublets arising from $^{109}Ag-^{31}P$ (647 Hz) and $^{107}Ag-^{31}P$ (560 Hz) one-bond coupling.

Similarly to the gold and copper complexes, the simple ^1H and ^{13}C NMR spectra indicate molecular C_5 symmetry for all three complexes **3a**−**c** arising from either static η^5 coordination or fast metallotropic isomerization. Complexes **3a**−**c** are unusual in that two doublets are clearly visible in the $^{31}P\{^1H\}$ NMR spectra (Figure 3), arising from $^1J(^{109}Ag-^{31}P)$ and $^1J(^{107}Ag-^{31}P)$ couplings (**3a**, 637 and 552 Hz, respectively; **3b**, 647 and 560 Hz, respectively; **3c**, 633 and 548 Hz, respectively). In general, the phosphorus resonances in unhindered complexes appear as broad singlets at room temperature because of fast ligand exchange.[24] A further indication that the observed doublets are due to silver−phosphorus coupling is shown by the $^1J(^{109}Ag-^{31}P)/^1J(^{107}Ag-^{31}P)$ ratio, which corresponds to the quotient of the gyromagnetic ratios for ^{109}Ag and ^{107}Ag (1.15).[24a] Even with complex **3b**, where the triphenylphosphine ligand is not as bulky as tricyclohexylphosphine, the crowded environment around the metal center impedes fast ligand exchange.

Interestingly, compounds **3a**−**c** are relatively air stable and can be manipulated at 20 °C. This is in stark contrast to the reported instability of parent complex $CpAg(PPh_3)$, which decomposes within minutes at 20 °C under inert atmosphere.[22] The enhanced stability is presumably due to steric shielding provided by the large aryl groups of fulleride ligands **1a** and **1b** and is consistent with reports that silver(I) phosphine complexes can be stabilized with substituted cyclopentadienyls.[22b] Accordingly, single crystals of **3a** and **3b** could be grown under argon at 20 °C in the dark over several days.

Representations of the crystal structures of **3a** and **3b** are shown in Figure 4, and crystallographic dimensions are collected in Table 1. Slow diffusion of *n*-pentane into a solution of **3a** in

dx.doi.org/10.1021/ja201297r |*J. Am. Chem. Soc.* 2011, 133, 6841–6851

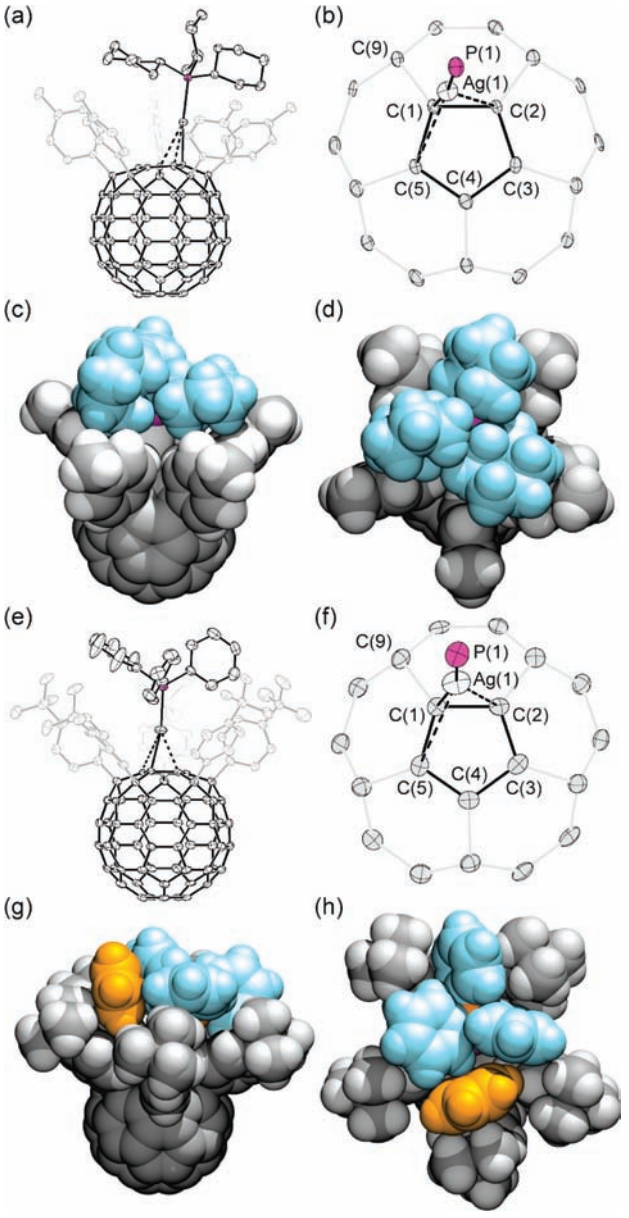

Figure 4. Representations of the crystal structures of $\mathbf{3a}\cdot(C_5H_{12})_{0.6}(C_2H_2Cl_4)_3$ (a–d) and $\mathbf{3b}\cdot(C_4H_8O)_{0.5}(C_6H_6)_{0.5}$, molecule **3b(A)** (e–h). (a) ORTEP drawing (thermal ellipsoids at 50% probability) of compound **3a**. (b) Partial structure of **3a** showing the metal–ligand bonding. (c, d) Space-filling representations of compound **3a**, viewed approximately parallel and perpendicular to the bonding cyclopentadienyl ring. (e) ORTEP drawing (thermal ellipsoids at 50% probability) of compound **3b(A)**. (f) Partial structure of **3b(A)** showing the ligand–metal bonding. (g, h) Space-filling representations of compound **3b(A)**, viewed approximately parallel and perpendicular to the bonding cyclopentadienyl ring. Hydrogen atoms are omitted for clarity in panels a and e.

1,1,2,2-tetrachloroethane resulted in the formation of single crystals of a solvate with $\mathbf{3a}\cdot(C_5H_{12})_{0.6}(C_2H_2Cl_4)_3$ stoichiometry. The extended crystal packing structure of **3a** has no eye-catching features and there are no short intermolecular contacts.

Importantly, a distorted η^3 coordination with a significant deviation toward η^2 (i.e., η^2/η^3) is observed for complex **3a**, which is unexpected and different from the η^5 and η^3 coordination modes reported for complex $[C_5H_2(SiMe_3)_3]Ag[P(n\text{-}Bu)_3]$.[9] The change of coordination geometry is apparent from the small differences in interatomic distances (0.266(4) and 0.635(4) Å, respectively) between the principal metal–ligand interaction Ag(1)–C(1) (2.259(4) Å) and the secondary interactions Ag(1)–C(2) (2.525(4) Å) and Ag(1)–C(5) (2.894(4) Å). Furthermore, in comparison to the gold complexes **2a** and **2b** (Table 1), a reduction in the metal–ligand bond angles Ag(1)–C(1)–C(2) (82.7(2)°) and Ag(1)–C(1)–C(5) (100.8(2)°), together with a corresponding increase in the angle Ag(1)–C(1)–C(9) (113.8(3)°), illustrates an increase in hapticity of metal–ligand bonding from η^1 to η^3. The bond alternation within the cyclopentadienyl ring of the silver(I) complex **3a** is markedly reduced in comparison to the gold complexes **2a** and **2b**, lying between a bond-localized butadiene system and a π-delocalized cyclopentadienyl system with local C_5 symmetry. However, there is stronger preference for π-delocalization in **3a** compared to the gold(I) complexes **2a** and **2b** (Table 1). The POAV angles for the cyclopentadienyl carbon atoms C(1)–C(5) indicate that the curvature is distributed more equally between the five carbon atoms of this convex ligand compared to gold complexes **2a** and **2b**. Carbon C(1) has less sp^3 character (POAV = 10.2°), and the remaining atoms C(2) to C(5) have slightly higher sp^3 character (POAV = 4.8–7.9°). These angles indicate a geometry intermediate between the η^1/η^3 coordination of gold complexes **2a** and **2b** and the η^5 coordination of copper complexes **4a** and **4b**.

Slow diffusion of *n*-pentane into a THF/benzene solution of the *tert*-butyl derivative $[(4\text{-}t\text{-}BuC_6H_4)_5C_{60}]Ag(PPh_3)$ (**3b**) at room temperature in the dark resulted in the growth of crystals suitable for single-crystal X-ray diffraction analysis (Figure 4e–h).[23] Under these conditions, complex **3b** forms a solvate $(\mathbf{3b}\cdot(C_4H_8O)_{0.5}(C_6H_6)_{0.5})$ with two independent molecules in the unit cell, which are referred to as **3b(A)** and **3b(B)** in the following discussion. For each complex, an occluded solvent molecule resides within a narrow, shallow cavity between the PPh_3 unit and an adjacent 4-*tert*-butylphenylene group. In **3b(A)**, a benzene molecule is occluded, whereas in **3b(B)** the THF occluded molecule is disordered over two positions. The geometries of the two molecules are similar and only **3b(A)** is described (Table 1, Figure 4e–h). As found for the silver complex **3a** described above, a situation between η^2 and η^3 coordination is observed. In the case of **3b(A)** however, the distortion toward η^2 is more severe. There is a difference of 0.587(5) Å between the interatomic distances Ag(1)–C(2) and Ag(1)–C(5) (2.464(5) and 3.051(5) Å, respectively), which is significantly greater than the corresponding difference of 0.369(5) Å in **3a**. The distortion from η^3 to η^2 in **3b(A)** is also apparent from the large difference in bond angle (29.1(3)°) between the ligand–metal angles Ag(1)–C(1)–C(2) and Ag(1)–C(1)–C(5) (78.8(3)° and 107.9(3)°, respectively), compared to the corresponding difference of 18.1(2)° in **3a**. Thus, the hapticity is more accurately described as η^2 with a slight distortion toward η^3. Indeed, the Ag(1)–C(1) and Ag(1)–C(2) distances (2.288(4) and 2.464(5) Å, respectively) differ only by 0.176(5) Å, and the Ag(1)–C(3) and Ag(1)–C(5) distances (3.224(4) and 3.051(5) Å, respectively) only by 0.173(5) Å. However, although the metal–ligand distances indicate η^2 coordination, bond lengths and pyramidalization angles within the cyclopentadienyl ring are consistent with η^3 coordination and are similar to those of **3a**.

The coordination modes observed in the crystal structures of **3a** and **3b** are different from those previously reported for the complex $[C_5H_2(SiMe_3)_3]Ag[P(n\text{-}Bu)_3]$ (Figure 5).[9] In this complex, the asymmetric unit comprises two isomers with different coordination modes; one isomer displays η^5 coordination, the other η^3. The η^3

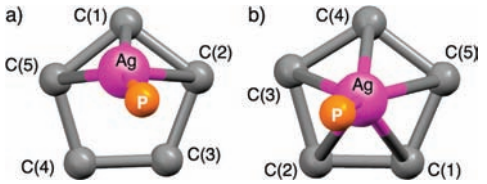

Figure 5. Representations of the crystal structure of $[C_5H_2(SiMe_3)_3]Ag[P(n\text{-}Bu)_3]$.[9] Views perpendicular to the (a) η^3- and (b) η^5-coordinated cyclopentadienyl rings of the complex.

isomer has higher hapticity ligand−metal bonding than is observed in compounds **3a** and **3b** in that it is distorted toward η^5 coordination with a longer, principal Ag(1)−C(1) interatomic distance (2.293(5) Å) and shorter, secondary interactions for Ag(1)−C(2) (2.421(5) Å) and Ag(1)−C(5) (2.644(5) Å). As discussed in the theoretical section below, the coordination preference of silver(I) in these complexes is intermediate between that of gold(I) and copper(I).

Copper(I) Complexes. Copper pentaarylfulleride complexes are of particular interest since the group of Nakamura has proposed them as intermediates in the copper(I)-mediated synthesis of pentaaryl hydrofullerenes.[10a] Sawamura et al. reported the complex $(Ph_5C_{60})Cu(PEt_3)$ synthesized *via* the reaction between $Ph_5C_{60}H$ and $(t\text{-}BuO)Cu(PEt_3)$. The ^1H and ^{13}C NMR spectra indicated apparent C_5 symmetry and the authors suggested η^5-coordination. However, considering the dearth of crystal structures of copper(I) cyclopentadienyl complexes and the possibility for fluxional processes showing higher apparent symmetry than that of the actual coordination geometry, we decided to investigate the (triphenyl phosphine)copper(I) pentaarylfulleride complexes derived from the ligand precursors **1a** and **1b**. Thus, the copper complex $[(4\text{-}MeC_6H_4)_5C_{60}]Cu(PPh_3)$ (**4a**) was synthesized *via* the reaction of $[ClCu(PPh_3)]_4$ with $K[(4\text{-}MeC_6H_4)_5C_{60}]$ (**1a**·K^+) in THF at −60 C.[23] HPLC analysis[23] of the reaction mixture indicated complete consumption of the fulleride starting material with concomitant formation of a single eluting product. Purification by chromatography on silica gel was not possible because of the high sensitivity of compound **4a** to air while bulk purification by crystallization was unsatisfactory. Rather, compound **4a** was purified by removal of THF in vacuo, followed by extraction with CS_2 and subsequent anaerobic filtration to remove salts and polar side products.

Single crystals of copper(I) complex **4a** were obtained by diffusion of *n*-pentane into a CS_2 solution at 20 °C in the dark over 7 days under argon. A similar reaction between $K[(4\text{-}t\text{-}BuC_6H_4)_5C_{60}]$ (**1b**·K^+) and $[ClCu(PPh_3)]_4$ afforded the complex $[(4\text{-}t\text{-}BuC_6H_4)_5C_{60}]Cu(PPh_3)$ (**4b**). In this case, it was possible to isolate compound **4b** in 65% yield *via* fast chromatography on a short silica gel column under argon and to obtain single crystals by slow diffusion of *n*-pentane into a solution of **4b** in $CHCl_3$. Single-crystal X-ray diffraction analyses were possible for both **4a** and **4b** (Figure 6).[23] Compounds **4a** and **4b** form solvates with **4a**·$(CS_2)_3$ and **4b**·$(CHCl_3)_3$ stoichiometry, respectively. Representations of the crystal structures are shown in Figure 6 and crystallographic dimensions are collected in Table 1.

The bonding in complexes **4a**·$(CS_2)_3$ and **4b**·$(CHCl_3)_3$ is essentially identical and can be described as pentahapto with a very slight deviation toward η^3 coordination. Thus, in **4a**·$(CS_2)_3$ the difference between the shortest and longest metal−ligand interatomic distances, Cu(1)−C(2) (2.171(2) Å) and Cu(1)−C(4) (2.352(2) Å), respectively, is 0.181(2) Å. The bond lengths within the

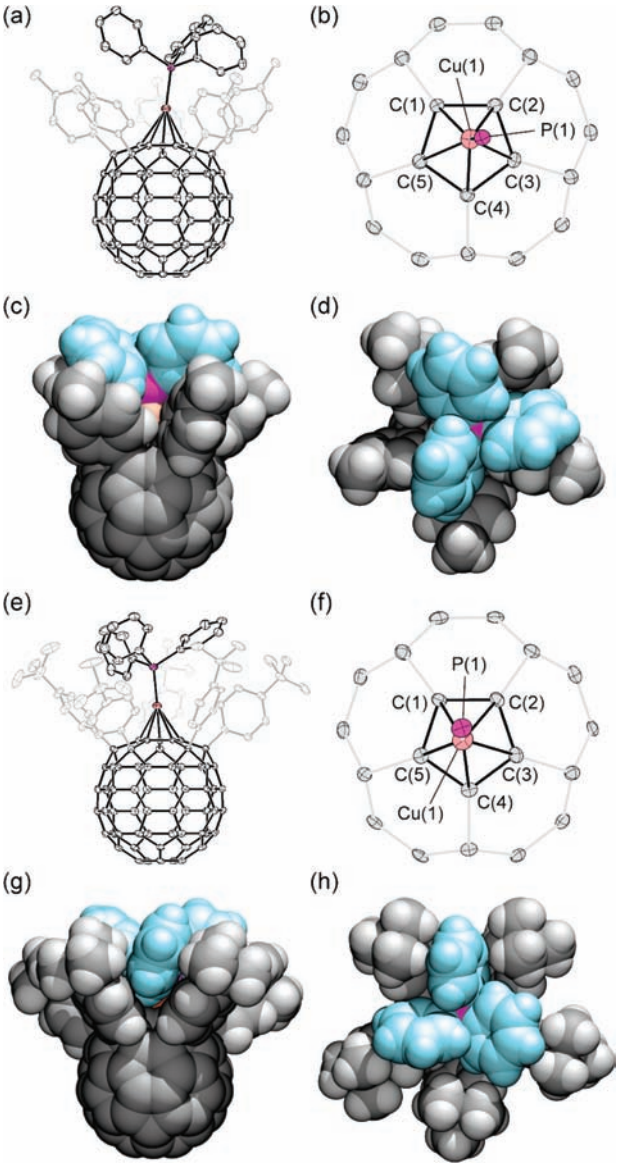

Figure 6. Representations of the crystal structures of **4a**·$(CS_2)_3$ (a−d) and **4b**·$(CHCl_3)_3$ (e−h). (a) ORTEP drawing (thermal ellipsoids at 50% probability) of compound **4a**. (b) Partial structure of **4a** showing the ligand−metal bonding. (c, d) Space-filling representations of compound **4a**, viewed approximately parallel and perpendicular to the bonding cyclopentadienyl ring. (e) ORTEP drawing (thermal ellipsoids at 50% probability) of compound **4b**. (f) Partial structure of **4b** showing the metal−ligand bonding. (g, h) Space-filling representations of compound **4b**, viewed approximately parallel and perpendicular to the bonding cyclopentadienyl ring. Hydrogen atoms are omitted for clarity in panels a and e.

cyclopentadienyl ring vary only to a small degree (max deviation of 0.012 Å in the case of **4a**·$(CS_2)_3$) and the pyramidalization angles of the carbon atoms of the cyclopentadienyl ring are nearly equal. These variations in bond lengths and angles are comparable to those of pentahapto "buckyferrocenes", e.g., $(\eta^5\text{-}C_{60}Me_5)FeCp$,[12d] and also to those of other copper(I) cyclopentadienyl phosphine complexes.[7]

Comparison of the whole series of crystal structures (Table 1) reveals that the shortest Ag−C interatomic distances (2.259(4)−2.288(4) Å) are significantly longer than the corresponding shortest Au−C distances (2.155(4)−2.176(4) Å).

dx.doi.org/10.1021/ja201297r |*J. Am. Chem. Soc.* 2011, 133, 6841–6851

Table 3. DFT-Calculated Interatomic Distances and Bond Angles for Simplified Models of Fullerenyl and Cyclopentadienyl Gold(I), Silver(I), and Copper(I) Phosphine Complexes Using the PBE Hybrid Functional with the 6-31G(d) Basis Set for H, C, and P, and the Stuttgart/Dresden ECP Plus DZ (SDD) Basis Set for Au, Ag, and Cu

	metal							
	Au		Au		Ag		Cu	
coordination	η^1	η^2	η^1	η^2	η^3	η^5	η^5	η^5
Cp ligand	H_5C_{60}	H_5C_{60}	Cp	Cp	H_5C_{60}	Cp	H_5C_{60}	Cp
phosphine	PH_3	PH_3	PH_3	PH_3	PH_3	PH_3	PH_3	PH_3
	Interatomic Distances (Å)							
M(1)−P(1)	2.299	2.272	2.296	2.257	2.350	2.300	2.140	2.128
M(1)−C(1)	2.126	2.276	2.115	2.278	2.212	2.460	2.223	2.210
M(1)−C(2)	2.775	2.978	2.770	2.910	2.562	2.465	2.226	2.211
M(1)−C(3)	3.408	3.318	3.467	3.229	3.007	2.468	2.223	2.212
M(1)−C(4)	3.408	2.978	3.465	2.910	3.008	2.465	2.226	2.211
M(1)−C(5)	2.775	2.276	2.768	2.278	2.565	2.460	2.223	2.211
C(1)−C(2)	1.481	1.423	1.467	1.420	1.448	1.423	1.423	1.423
C(2)−C(3)	1.374	1.401	1.374	1.404	1.405	1.423	1.423	1.423
C(3)−C(4)	1.430	1.401	1.434	1.404	1.410	1.423	1.423	1.423
C(4)−C(5)	1.374	1.423	1.374	1.420	1.405	1.423	1.423	1.423
C(5)−C(1)	1.481	1.472	1.467	1.458	1.448	1.423	1.423	1.423
	Bond Angles (deg)							
P(1)−M(1)−C(1)	179.4	161.1	179.7	161.3	176.8	150.8	147.3	147.1
M(1)−C(1)−C(2)	99.0	104.9	99.7	101.2	86.2	73.4	71.5	71.3
M(1)−C(1)−C(5)	99.0	71.1	99.6	71.3	86.3	73.2	71.3	71.2

Because the coordination of the cyclopentadienyl ring to each of these two metal centers is similar, the differences in interatomic distances reflect the greater covalent radii of silver (1.45 Å) relative to gold (1.36 Å).[25] However, although the covalent radius of copper (1.32 Å) is less than that of gold, the shortest Cu−C distances (2.171(2) and 2.190(4) Å) are slightly longer than those of the Au complexes because the higher coordination of the cyclopentadienyl ring to copper(I) (η^5) results in an elongation of the shortest metal−carbon bonds.

Pentahapto bonding in cyclopentadienyl systems has been rationalized using molecular orbital theory.[19] Although the cationic $Au(PPh_3)^+$, $Ag(PPh_3)^+$ and $Cu(PPh_3)^+$ fragments are isolobal, they vary greatly with respect to the relative energies of their orbitals and the extent to which they can interact with the molecular orbitals of the anionic cyclopentadienyl fragment. Thus, unlike the $6p_x$ and $6p_y$ orbitals of the $Au(PR_3)^+$ fragment described above, the vacant, degenerate $4p_x$ and $4p_y$ orbitals of the $Cu(PPh_3)^+$ fragment are energetically well matched with the filled cyclopentadienyl-based orbitals, and together they participate in stabilizing bonding interactions. Furthermore, relative to the $Au(PPh_3)^+$ fragment, the filled d orbitals of the $Cu(PPh_3)^+$ fragment are low in energy and do not engage in destabilizing interactions with the filled cyclopentadienyl-based orbitals. Together, these factors stabilize pentahapto bonding relative to lower coordination modes.

DFT Calculations. We carried out density functional theory (DFT) calculations using Gaussian 09,[23,26] examining the model system $(H_5C_{60})M(PH_3)$ (M = Au, Ag, Cu) to evaluate energetic and geometric aspects of the bonding modes in these complexes. The cyclopentadienyl system $CpMPH_3$ (M = Au, Ag, Cu) was also calculated for comparison. We used the exact-exchange-incorporated PBE hybrid functional with a 6-31G(d) basis set for H, C, P and the Stuttgart/Dresden ECP plus DZ (SDD) basis set for Au, Ag, and Cu because this level of theory has been studied comparatively and this method reproduces the geometry of third row transition metal complexes reasonably well.[27b] We were also interested in determining whether the convexity of the cyclopentadienyl ligand in the fulleride complexes has an influence on metal−ligand bonding interactions. The simplified fulleride model $(H_5C_{60})M(PH_3)$ (M = Au, Ag, Cu) avoids potential steric influences by larger substituents on the coordination geometry, which is important in view of the small energy differences that can exist between different coordination modes in these systems.[27a] With the larger model $(Ph_5C_{60})M(PPh_3)$ (M = Au, Ag, Cu), the bulky phenyl groups can have a dramatic influence on the calculated geometry, resulting in unexpected geometries.[28]

Gold(I) Complexes. The minimum for $CpAuPH_3$ corresponds to a symmetrical η^1 coordination with a marked bond alternation within the cyclopentadienyl ring (Table 3).[23] Additionally, an η^2-coordinated species with a relative energy of +2.4 kcal/mol after zero-point energy correction was found as a transition state linking the two equivalent η^1-coordinated minima. These results are consistent with previous computational results,[27a] crystallographic data,[8] and the results of our NMR spectroscopy experiments, which indicate a time-averaged C_s symmetry resulting from fast $\eta^1 \rightarrow \eta^2 \rightarrow \eta^1$ metallotropic rearrangement. Analogously, the energy difference between the η^1 minimum and the η^2 transition state of the "bare" fulleride model $(H_5C_{60})Au(PH_3)$ is only +2.3 kcal/mol after zero-point energy correction, indicating that, for this gold(I) model, the convex nature of the cyclopentadienyl ligand does not have a visible influence on the distortion of the complex between the η^1 and η^2 coordination states.

dx.doi.org/10.1021/ja201297r | J. Am. Chem. Soc. 2011, 133, 6841–6851

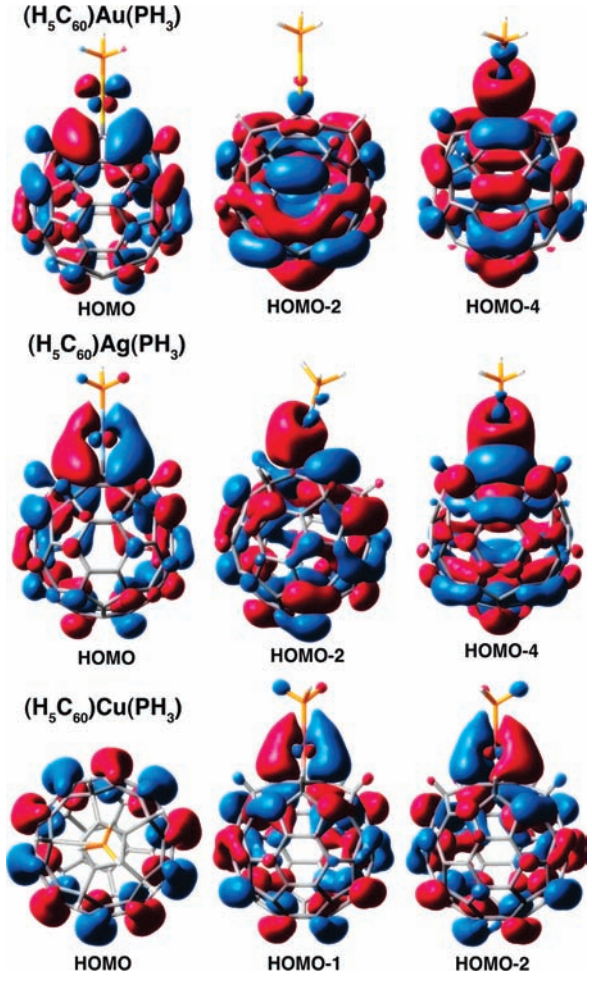

Figure 7. Selected molecular orbitals for $(H_5C_{60})Au(PH_3)$, $(H_5C_{60})Ag(PH_3)$, and $(H_5C_{60})Cu(PH_3)$ plotted with an isovalue of 0.015.

Silver(I) Complexes. Previously reported computational studies[27a] on the simplified system $CpAgPH_3$ indicated that, although η^5 coordination is a minimum, the potential energy surface with respect to ring slippage is broad and shallow, and a range of coordination modes are accessible within a few kcal/mol including η^1 and η^2. Since there is a discrepancy between the optimized structure of $CpAgPH_3$ and the solid-state structures of **3a** and **3b**, the fullerene-based model system $(H_5C_{60})Ag(PH_3)$ was also calculated. Confirming the earlier findings,[27a] the minimum for $CpAgPH_3$ has η^5 coordination (Table 3). In contrast, the minimum for $(H_5C_{60})Ag(PH_3)$ has η^3 coordination with a principal Ag−C interaction of 2.212 Å and two secondary Ag−C interactions of 2.562 and 2.565 Å, indicating that the convexity of the fulleride-based cyclopentadienyl ligand may play a role in the coordination of this model system.

Copper(I) Complexes. In previous computational work,[27a] the global minimum located for the model system $CpCuPH_3$ had η^5 coordination. The potential energy curve with respect to ring slippage was found to be steep and narrow, contrary to that of the analogous silver(I) complex. Our DFT calculations reproduce these results.[23,27a] The minimum for $CpCuPH_3$ has η^5 coordination, with nearly equal bond distances between Cu(I) and the five carbon atoms C(1) to C(5) of the cyclopentadienyl ligand (Table 3). The fulleride model $(H_5C_{60})Cu(PH_3)$ has similar geometry, but with slightly elongated bonds (0.012−0.015 Å) between Cu(I) and the five carbon atoms C(1) to C(5) compared to $CpCuPH_3$. The calculated structures for both models reproduce the experimental interatomic distances for complexes **4a** and **4b**. For example, the five interatomic distances between Cu(I) and carbon atoms C(1) to C(5) in $(H_5C_{60})Cu(PH_3)$ average 2.224 Å (Table 3), compared to the experiment averages of 2.2642(2) and 2.2716(4) Å for **4a** and **4b**, respectively (Table 1). The distances between the carbons within cyclopentadienyl units for both models are nearly identical (1.423 Å). The calculations reproduce the averaged experimentally observed values for **4a** and **4b** (1.4244(3) and 1.4206(5) Å, respectively), and underline the delocalized aromatic nature of the fulleride-based cyclopentadienyl ligand observed experimentally in these two complexes.

Frontier Molecular Orbitals. The frontier molecular orbitals of the gold(I) and silver(I) model complexes share similar features (Figure 7 and Supporting Information).[23] In particular, the HOMOs of the fulleride-based models $(H_5C_{60})Au(PH_3)$ and $(H_5C_{60})Ag(PH_3)$ have strong contributions from the corresponding cyclopentadienide π orbital, with small antibonding contributions from the $5d_{x2-y2}$ gold orbital and the $4d_{x2-y2}$ silver orbital. The HOMO-4 for $(H_5C_{60})Au(PH_3)$ is mainly a σ orbital between gold and the cyclopentadienyl carbon C(1).[23] The HOMO-2 and HOMO-4 for the silver(I) model $(H_5C_{60})Ag(PH_3)$ are similar, while for the gold(I) model there is much less σ bond contribution in the HOMO-2 compared to the HOMO-4.

In contrast, the fulleride copper model complex $(H_5C_{60})Cu(PH_3)$ shows contributions of copper 4p and 3d orbitals to bonding in the HOMO-1 and HOMO-2, as one would expect from the η^5-coordination geometry of this complex (Figure 7). The HOMO of the model copper complex $(H_5C_{60})Cu(PH_3)$ is a quasi-C_5-symmetric fullerene-based orbital.

CONCLUSION

The pentaarylfulleride ligand **1**, as represented by its specific derivatives **1a** and **1b**, is highly effective in stabilizing group 11 metal complexes (**2a**, **2b**, **4a**, **4b**, **3a**, **3b**, and **3c**). It is clear that the steric shielding provided by the aryl substituents on ligands **1a** and **1b**, in addition to that from triphenylphosphine or tricyclohexylphosphine, is an important factor in the successful isolation and crystallographic characterization of an underrepresented family of phosphine cyclopentadienyl complexes. These new compounds are also the first examples of fullerene complexes of gold(I), silver(I), and copper(I) to be crystallographically characterized. The gold(I) complexes **2a** and **2b** coordinate the fulleride-based cyclopentadienyl anion to the metal in an η^1 fashion, whereas in the case of $\mathbf{2a}\cdot(CHCl_3)_2(CS_2)$ there is distortion of the complex toward η^2 coordination that is presumably due to crystal packing forces. On the other hand, pentahapto bonding characterizes the fulleride copper complexes **4a** and **4b**, as is typical for phosphine copper(I) cyclopentadienyl complexes. The η^2/η^3-type bonding observed in the silver complexes **3a** and **3b**, together with the previously reported η^3 and η^5 bonding in the structure of $[C_5H_2(SiMe_3)_3]Ag[P(n\text{-}Bu)_3]$,[9] shows that a range of coordination modes is easily accessible in the phosphine silver(I) cyclopentadienyl family due to the small energy changes accompanying these distortions.

The DFT calculations reproduce interatomic distances and bond angles observed experimentally, and provide insight into

the electronic structures of these complexes. Bonding to the fulleride ligand is dominated by orbital availability, as has been previously shown, with a subtle influence from the pyramidalization of the cyclopentadienyl carbons on the coordination of the Au(I), Ag(I), and Cu(I) cations. The influence of pyramidalization is strongest in the silver(I) complexes. All these effects work synergistically to modulate orbital overlap between gold(I), silver(I), or copper(I) and the fullerene cyclopentadienyl orbitals.

Thus, the inherent angle strain affecting all carbons of the fullerene-embedded cyclopentadienyl ring may have significant implications regarding the coordinating properties of ligands **1a** and **1b**. This strain is imparted primarily by the spherical nature of the fullerene cage and results in the pyramidalization of the cyclopentadienyl carbons in all pentaarylfulleride complexes (Chart 1b). Interestingly, for unstrained nonfullerenyl cyclopentadienyl complexes, the substituents tilt either toward the metal (hydrogens of Cp) as a result of a slight rehybridization of the trigonal carbons leading to increased ligand−metal orbital overlap or away for methyl groups and other larger substituents due to supplementary steric factors.[29] On the other hand, the cyclopentadienyl π orbitals in the fulleride ligands **1a** and **1b** are aligned radially with respect to the C_{60} cage because of the convex shape of the embedded cyclopentadienyl moiety, rather than perpendicularly to the plane of the Cp ring (Chart 1). As a result of this unusual orientation, the 2p orbitals cannot interact as efficiently with the d orbitals of a metal center in the η^5 coordination geometry. This is most clearly seen experimentally with unusually distinctive ligand−metal distances in the "dual" fulleroferrocene complex (η^5-$C_{60}Me_5$)Fe(η^5-C_5H_5), which has both fulleride-based and Cp cyclopentadienyl ligands: the averaged C−Fe bond length between the Me_5C_{60} carbons and iron(II) is 2.089 Å, whereas it is significantly shorter (2.033 Å) between the Cp carbons and iron(II).[12d,30]

It is important to note that the crystallographically characterized, noncoordinated metal fulleride salts $[Li(THF)_4][Ph_5C_{60}]$ or $[Zr(NMe_2)_3(THF)_2][Ph_5C_{60}]$[12m] have a similar curvature, as shown by the averaged POAV values for the cyclopentadienyl carbons (6.2 and 6.2, respectively). These values are comparable to the POAV values of the sp^2-hybridized carbons C(2)−C(5) in complexes **2a,b**, **3a,b**, or **4a,b**, which range from 4.3 to 7.9 (Table 1). Interestingly, this curvature does not change significantly upon metal ligation.

However, at a localized level, the angle strain resulting from pyramidalization of the fulleride cyclopentadienyl ring carbons is distributed between all five atoms in the case of symmetrical η^5 bonding (copper(I)). On the other hand, in the case of σ bonding (η^1-coordination), for example, in $C_{60}Ph_5Me$ or $(H_5C_{60})Au(PH_3)$, four formally sp^2-hybridized cyclopentadienyl carbons are now significantly planarized, while the remaining sp^3-hybridized C(1) carbon atom is significantly pyramidalized, which reduces its hybridization strain and stabilizes the overall complex. Within the series of complexes described in this work, the copper(I) complexes **4a** and **4b** represent one extreme of the bonding spectrum, in which the increase in stability associated with pentahapto bonding over σ/η^1 bonding more than compensates for the destabilization associated with the greater angle strain at carbons C(1)−C(5). The gold complexes **2a** and **2b** represent the other extreme, in which no stabilization is gained through pentahapto bonding and the complex adopts η^1 coordination. The silver complexes **3a** and **3b** are interesting intermediate cases, in which the relief of angle strain is in close competition with the stabilizing effect of pentahapto bonding. This combination of factors results in the intermediate η^2/η^3 coordination.

Accordingly, the greatly increased stability of metal complexes resulting from the steric shielding imparted by the aryl groups of fulleride anions **1a** and **1b** bodes well for the isolation of other unstable transition metal complexes and even some reactive species.[31] Further work in this direction will be reported in due time.

■ ASSOCIATED CONTENT

Supporting Information. Spectroscopic characterization data for compounds **3a**−**c** and **4a,b**. Crystallographic information files in CIF format for **3a**·$(C_5H_{12})_{0.6}(C_2H_2Cl_4)_3$, **3b**·$(C_4H_8O)_{0.5}(C_6H_6)_{0.5}$, **4a**·$(CS_2)_3$, and **4b**·$(CHCl_3)_3$. Computational details, frontier orbital representations, and atom coordinates for the minimized structures. This material is available free of charge via the Internet at http://pubs.acs.org.

■ AUTHOR INFORMATION

Corresponding Author
rubin@chem.ucla.edu

■ ACKNOWLEDGMENT

We are grateful to the National Science Foundation, the Office of Naval Research, and the U.S. Department of Energy, Office of Basic Energy Sciences as part of an Energy Frontier Research Center, for financial support with research grants NSF-CHE-0527015, NSF-CHE-0911758, ONR-N00014-04-1-0410, and DOE-BES (EFRC DE-SC0001342) for Y.R., the Sloan Foundation for P.L.D., and the NSF for instrumentation grants NSF-CHE-9871332 (X-ray) and NSF-CHE-9974928 (NMR).

■ REFERENCES

(1) Van Peski, A. J.; Melsen, J. A. U.S. Patent 2,150,349, 1938.
(2) Kealy, T. J.; Pauson, P. L. *Nature* **1951**, *168*, 1039–1040. Wilkinson, G.; Rosenblum, M.; Whiting, M. C.; Woodward, R. B. *J. Am. Chem. Soc.* **1952**, *74*, 2125–2126.
(3) Wilkinson, G.; Piper, T. S. *J. Inorg. Nucl. Chem.* **1956**, *2*, 32–37.
(4) Cotton, F. A.; Marks, T. J. *J. Am. Chem. Soc.* **1969**, *91*, 7281–7285.
(5) (a) Cotton, F. A.; Takats, J. *J. Am. Chem. Soc.* **1970**, *92*, 2353–2358. (b) Delbaere, L. T. J.; McBride, D. W.; Ferguson, R. B. *Acta Crystallogr.* **1970**, *B26*, 515–521.
(6) Jutzi, P.; Wieland, W.; Neumann, B.; Stammler, H.-G. *J. Organomet. Chem.* **1995**, *501*, 369–374.
(7) (a) Hanusa, T. P.; Ulibarri, T. A.; Evans, W. J. *Acta Crystallogr.* **1985**, *C41*, 1036–1038. (b) Anderson, Q. T.; Erkizia, E.; Conry, R. R. *Organometallics* **1998**, *17*, 4917–4920. (c) Carriedo, G. A.; Howard, J. A. K.; Stone, F. G. A. *J. Chem. Soc., Dalton Trans.* **1984**, 1555–1561. (d) Zybill, C.; Müller, G. *Organometallics* **1987**, *6*, 2489–2494. (e) Ren, H; Zhao, X.; Xu, S.; Song, H.; Wang, B. *J. Organomet. Chem.* **2006**, *691*, 4109–4113. (f) Olbrich, F.; Schmidt, G.; Weiss, E.; Behrens, U. *J. Organomet. Chem.* **1993**, *456*, 299–303. (g) Johnson, A. L.; Willcocks, A. M.; Raithby, P. R.; Warren, M. R.; Kingsley, A. J.; Odedra, R. *Dalton Trans.* **2009**, 922–924.
(8) (a) Perevalova, E. G.; Grandberg, K. J.; Dyadchenko, V. P.; Baukova, T. V. *J. Organomet. Chem.* **1981**, *217*, 403–413. (b) Baukova, T. V.; Slovokhotov, Yu. L.; Struchkov, Yu. T. *J. Organomet. Chem.* **1981**, *220*, 125–137. (c) Bruce, M. I.; Walton, J. K.; Skelton, B. W.; White, A. H. *J. Chem. Soc., Dalton Trans.* **1983**, 809–814. (d) Werner, H.; Otto, H.; Ngo-Khac, T.; Burschka, Ch. *J. Organomet. Chem.* **1984**, *262*, 123–136. (e) Struchkov, Yu. T.; Slovokhotov, Yu. L.; Kravtsov,

D. N.; Baukova, T. V.; Perevalova, E. G.; Grandberg, K. J. *J. Organomet. Chem.* **1988**, *338*, 269–280. (f) Schumann, H.; Görlitz, F. H.; Dietrich, A. *Chem. Ber.* **1989**, *122*, 1423–1426. (g) Bruce, M. I.; Humphrey, P. A.; Williams, M. L.; Skelton, B. W.; White, A. H. *Aust. J. Chem.* **1989**, *42*, 1847–1857. (h) Kuz'mina, L. G.; Churakov, A. V.; Grandberg, K. I.; Kuz'min, V. S. *Koord. Khim.* **1997**, *23*, 170–176.

(9) Stammler, H.-G.; Jutzi, P.; Wieland, W.; Neumann, B. *Acta Crystallogr.* **1998**, *C54*, IUC9800064.

(10) (a) Matsuo, Y.; Nakamura, E. *Chem. Rev.* **2008**, *108*, 3016–3028. (b) Sawamura, M.; Iikura, H.; Ohama, T.; Hackler, U. E.; Nakamura, E. *J. Organomet. Chem.* **2000**, *599*, 32–36.

(11) The majority of metal complexes of fullerenes involve eta-2 coordination; see: (a) Balch, A. L.; Olmstead, M. M. *Chem. Rev.* **1998**, *98*, 2123–2165. (b) Yeh, W.-Y.; Tsai, K.-Y. *Organometallics* **2010**, *29*, 604–609 and references therein.

(12) (a) Sawamura, M.; Iikura, H.; Nakamura, E. *J. Am. Chem. Soc.* **1996**, *118*, 12850–12851. (b) Matsuo, Y.; Iwashita, A.; Nakamura, E. *Organometallics* **2008**, *27*, 4611–4617. (c) Matsuo, Y.; Kuninobu, Y.; Muramatsu, A.; Sawamura, M.; Nakamura, E. *Organometallics* **2008**, *27*, 3403–3409. (d) Sawamura, M.; Kuninobu, Y.; Toganoh, M.; Matsuo, Y.; Yamanaka, M.; Nakamura, E. *J. Am. Chem. Soc.* **2002**, *124*, 9354–9355. (e) Nakamura, E. *J. Organomet. Chem.* **2004**, *689*, 4630–4635. (f) Matsuo, Y.; Kuninobu, Y.; Ito, S.; Nakamura, E. *Chem. Lett.* **2004**, *33*, 68–69. (g) Matsuo, Y.; Nakamura, E. *Organometallics* **2003**, *22*, 2554–2563. (h) Herber, R. H.; Nowik, I.; Matsuo, Y.; Toganoh, M.; Kuninobu, Y.; Nakamura, E. *Inorg. Chem.* **2005**, *44*, 5629–5635. (i) Matsuo, Y.; Mitani, Y.; Zhong, Y.-W.; Nakamura, E. *Organometallics* **2006**, *25*, 2826–2832. (j) Matsuo, Y.; Iwashita, A.; Nakamura, E. *Organometallics* **2005**, *24*, 89–95. (k) Sawamura, M.; Kuninobu, Y.; Nakamura, E. *J. Am. Chem. Soc.* **2000**, *122*, 12407–12408. (l) Kuninobu, Y.; Matsuo, Y.; Toganoh, M.; Sawamura, M.; Nakamura, E. *Organometallics* **2004**, *23*, 3259–3266. (m) Bouwkamp, M. W.; Meetsma, A. *Inorg. Chem.* **2009**, *48*, 8–9.

(13) Halim, M.; Kennedy, R. D.; Khan, S. I.; Rubin, Y. *Inorg. Chem.* **2010**, *49*, 3974–3976.

(14) (a) Haddon, R. C. *J. Am. Chem. Soc.* **1997**, *119*, 1797–1789. (b) Haddon, R. C. *J. Phys. Chem. A* **2001**, *105*, 4164–4165.

(15) Hamilton, E. J. M.; Welch, A. J. *Polyhedron* **1990**, *9*, 2407–2412.

(16) (a) Gavens, P. D.; Guy, J. J.; Mays, M. J.; Sheldrick, G. M. *Acta Crystallogr.* **1977**, *B33*, 137–139. (b) Liu, L.-K.; Luh, L.-S.; Wen, Y-S; Eke, U. B.; Mesubi, M. A. *Organometallics* **1995**, *14*, 4474–4482.

(17) Zhong, Y.-W.; Matsuo, Y.; Nakamura, E. *Org. Lett.* **2006**, *8*, 1463–1466.

(18) Hoffmann, R. *Angew. Chem., Int. Ed.* **1982**, *21*, 711–724.

(19) (a) Mingos, D. M. P.; Forsyth, M. I.; Welch, A. J. *J. Chem. Soc., Dalton Trans.* **1978**, 1363–1374. (b) Evans, D. G.; Mingos, D. M. P. *J. Organomet. Chem.* **1982**, *232*, 171–191.

(20) Ferguson, G.; Gallagher, J. F.; Kennedy, J. D.; Kelleher, A.-M.; Spalding, T. R. *Dalton Trans.* **2006**, 2133–2139.

(21) Bruce, M. I.; Williams, M. L.; Skelton, B. W.; White, A. H. *J. Chem. Soc., Dalton Trans.* **1983**, 799–808.

(22) (a) Hofstee, H. K.; Boersma, J.; van der Kerk, G. J. M. *J. Organomet. Chem.* **1976**, *120*, 313–317. (b) Lettko, L.; Rausch, M. D. *Organometallics* **2000**, *19*, 4060–4065.

(23) See Supporting Information.

(24) (a) Dias, H. V. R.; Jin, W.; Kim, H.-J.; Lu, H.-L. *Inorg. Chem.* **1996**, *35*, 2317–2328. (b) Dias, H. V. R.; Singh, S. *Inorg. Chem.* **2004**, *43*, 7396–7402.

(25) Cordero, B.; Gómez, V.; Platero-Prats, A. E.; Revés, M.; Echeverría, Cremades, E.; Barragán, F.; Alvarez, S. *Dalton Trans.* **2008**, 2832–2838.

(26) Frisch, M. J. et al. *Gaussian 09, Revision A.02*; Gaussian Inc.: Wallingford, CT, 2009. See Supporting Information for the full citation of Gaussian 09 and computational details.

(27) (a) Budzelaar, P. H. M.; Engelberts, J. J.; van Lenthe, J. H. *Organometallics* **2003**, *22*, 1562–1576. (b) Bühl, M.; Reimann, C.; Pantazis, A. D.; Bredow, T.; Neese, F. *J. Chem. Theory Comput.* **2008**, *4*, 1449–1459.

(28) DFT calculations carried out on the series of metal complexes $(Ph_5C_{60})M(PPh_3)$ (M = Au, Ag, Cu) using ADF 2009 (Local Density Approximation by Becke-Perdew with Triple-ζ STA Basis Sets for Au, Ag, Cu, and P) gave geometries similar to those referred to in Table 3 in the case of $(Ph_5C_{60})Au(PPh_3)$ (η^1) and $(Ph_5C_{60})Ag(PPh_3)$ (η^2/η^3). However, the geometry optimization of $(Ph_5C_{60})Cu(PPh_3)$ resulted in η^1 coordination; see ref 23.

(29) See for example: (a) Haaland, A. *Acc. Chem. Res.* **1979**, *12*, 415–422. (b) Glöckner, A.; Tamm, M.; Arif, A. M.; Ernst, R. D. *Organometallics* **2009**, *28*, 7041–7046.

(30) Nakamura, E. *Pure Appl. Chem.* **2003**, *75*, 427–434.

(31) (a) Warmuth, R.; Yoon, J. *Acc. Chem. Res.* **2001**, *34*, 95–105. (b) Hof, F.; Craig, S. L.; Nuckolls, C.; Rebek, J., Jr. *Angew. Chem., Int. Ed.* **2002**, *41*, 1488–1508.